

## THERMAL ANALYSIS OF Cu(II) IMIDAZOLE COORDINATION COMPOUNDS

J.G. VAN BERKUM \* and G. HAKVOORT

*Department of Chemistry, Delft University of Technology, P.O. Box 5045, 2600 GA Delft (The Netherlands)*

J. REEDIJK

*Department of Chemistry, Gorlaeus Laboratories, State university Leiden, P.O. Box 9502, 2300 RA Leiden (The Netherlands)*

(Received 24 June 1980)

### ABSTRACT

Thermal decomposition reactions of compounds  $\text{Cu}(\text{LH})_n\text{X}_2$ , with LH = imidazole (IzH) and *N*-methyl imidazole (NMeIzH),  $n = 2, 4$  and X = Cl, Br, have been studied with the aid of thermogravimetric analysis (TG), mass spectroscopy (MS), high-temperature X-ray powder diffraction and differential scanning calorimetry (DSC).

Only in a few cases could simple ligand losses be studied. In most cases a simultaneous ligand loss and redox reaction occurred, resulting in CuCl (or CuBr) and finally Cu metal. One of the oxidation products could be characterized by mass spectroscopy and appeared to be chlorinated imidazoles. This relative stabilization of Cu(I) by imidazole ligands corresponds with known synthetical chemistry. No accurate binding enthalpies for the imidazole ligands could be deduced.

### INTRODUCTION

The binding between metal(II) ions and imidazole ligands frequently occurs in nature, as many metalloproteins are coordinated by the imidazole side chains of histidyl residues. Examples are superoxide dismutase [1], haemoglobin [2], myoglobin [3], and cytochrome-c [4]. The formation and reactivity of the metal–imidazole bond has been the subject of many investigations [5]. Metal coordination compounds containing imidazole ligands have been synthesized for many years, and have been studied intensively both structurally and spectroscopically [6–9]. So far, the number of thermochemical investigations on imidazole compounds has been limited, and in fact has been restricted to Ni(II) [10], Co(II) [11] and Pd(II) [12]. No thermal analytical studies of Cu(II), a metal which is known to coordinate to histidyl imidazole groups, have been reported so far. It is known that apart from the coordination bond between the metal ion and the

---

\* To whom correspondence should be addressed.

pyridine-nitrogen of imidazole, hydrogen-bond interaction of the N—H group also plays an important role in the stabilization of certain metallo-proteins. We therefore first studied the differences on going from imidazole [10] to *N*-methyl imidazole (without hydrogen bonding) [13] with respect to their coordination to Ni(II) as a standard. The present study deals with an investigation on the thermal behaviour of coordination compounds containing these ligands coordinated to copper, as a case which is closer to the naturally occurring systems. Because initial experiments showed very complicated decomposition reactions, we decided to compare imidazole and *N*-methyl imidazole under the same conditions and to analyze the decomposition products (as a function of temperature) also by high resolution mass spectroscopy.

## EXPERIMENTAL

### *Starting materials and synthesis*

Imidazole (IzH), *N*-methyl imidazole (NMeIzH) and copper salts were commercially available and used without purification. The compounds of general formula  $\text{Cu}(\text{LH})_n\text{X}_2$ , where LH = IzH, NMeIzH and  $n = 2, 4$  and X = Cl, Br, were prepared as described in previous investigations [14–16]. They were checked for purity by elemental analyses, IR spectroscopy and ligand field spectroscopy.

### *Thermogravimetry (TG)*

Thermogravimetric results were obtained using a thermobalance constructed in our laboratory [17] furnished with a C.I. Electronics microbalance. The samples were studied in Pt cups having a flat bottom (6 mm diameter) and a small raised border (2 mm). The weight of the samples varied from 1–8 mg. It is noticed that weights of 1–3 mg gave better results.

The reactions were carried out in a stream of high-purity helium (15–20 ml min<sup>-1</sup>) with a heating rate of 12°C min<sup>-1</sup>. The temperature was measured by a chromel–alumel thermocouple.

During heating both the temperature and the weight of the sample were registered by a recorder having a paper speed of 10 mm min<sup>-1</sup>. Before each experiment the whole apparatus was evacuated in order to prevent oxidation of the decomposition products by air during heating.

### *High-temperature Guinier photographs (HTRö)*

The diffraction patterns were obtained using a standard high-temperature Guinier–De Wolf camera, with  $\text{CuK}\alpha$  radiation. While the sample was continuously held under a nitrogen atmosphere the temperature was raised with 1.2°C min<sup>-1</sup>. This low heating was necessary, due to the sensitivity of the film material used.

The line patterns obtained as a function of temperature were compared

with known patterns [18]. As a result the solid intermediate and end products, obtained during heating of the sample, could be characterized.

### *Differential scanning calorimetry (DSC)*

To obtain calorimetric results a DSC delivered by Du Pont Instruments was used, consisting of a DSC-cell (type 910) and a thermal analyzer (type 990). The cell has been furnished with a platinum(II) control thermocouple and a chromel–alumel sample thermocouple.

Platinum cups were used as described in the TG experiments. The usual heating rate was 5 or 10°C min<sup>-1</sup> with a calorimetric sensitivity of either 0.67, 1.67, 3.35, 6.69 or 16.74 mJ s<sup>-1</sup> at full scale width. The instrument was calibrated by measuring the heat of fusion of a known amount of high-purity indium. Each DSC experiment was also checked on accuracy of time, resulting in an overall calibration coefficient  $E$ .

After evacuating the apparatus the samples were heated in a stream of high-purity helium with a flow rate of 15–20 ml min<sup>-1</sup>. The weight of the samples was 1–5 mg.

Heats of reaction were obtained with the relation

$$Q = E \int \Delta q \, dt = EA$$

in which  $Q$  = the heat of reaction in mJ;  $E$  = a dimensionless calibration coefficient;  $q$  = the heat flow in mJ s<sup>-1</sup>; and  $A$  = peak area expressed in mJ. If  $E$  is known the heat of reaction can be determined by measuring the peak area with a planimeter.

### *Mass spectroscopy (MS)*

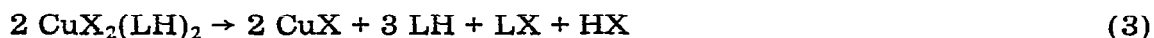
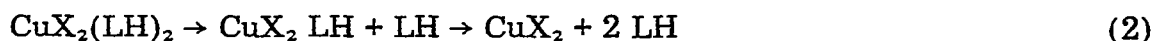
To analyze the gaseous decomposition products a mass spectrometer (Varian 311 A) was used, furnished with an open atmospheric split. A special glass tube was fitted. Through one end with an inner diameter of 6 mm containing the glass sample holder, a stream of helium was led with a flow rate of 10–15 ml min<sup>-1</sup>. The other end, narrowed to a capillary with an inner diameter of 1.3 mm, was fitted into an open atmospheric split as part of the mass spectrometer. The glass tube was heated in a furnace (heating rate 10°C min<sup>-1</sup>). Complete mass spectra were scanned every 10 s and on line converted to mass chromatograms of selected ions by a computer system (PDP 11/45). As a result gas chromatograms (GC) and evolved gas analysis curves (EGA) have been obtained. The GC curve can be interpreted as the amount of evolved gaseous products vs. temperature.

## RESULTS AND DISCUSSION

### *General*

From the experiments it can be concluded that the decomposition of the copper(II) imidazole and *N*-methyl imidazole chlorides and bromides can

generally be described by the following reactions



with X = Cl, Br and LH = IzH, NMeIzH.

In all experiments mass spectra showed the existence of the dihalogenated products, LX<sub>2</sub>, at the same temperature as LX was detected. However, in this discussion they will be neglected because the amounts formed during the decomposition seemed to be extremely small.

### *N-Methyl imidazole compounds*

Figure 1 shows the thermal decomposition of CuCl<sub>2</sub>(NMeIzH)<sub>2</sub>. The first DSC peak (at 152°C) represents the melting point of the compound with a slight loss of ligand. This can be concluded from the TG curve at 12°C min<sup>-1</sup> and the EGA curve of NMeIzH<sup>+</sup> (mass 82). The heat of melting is found to be 16 ± 1 kJ mole<sup>-1</sup>.

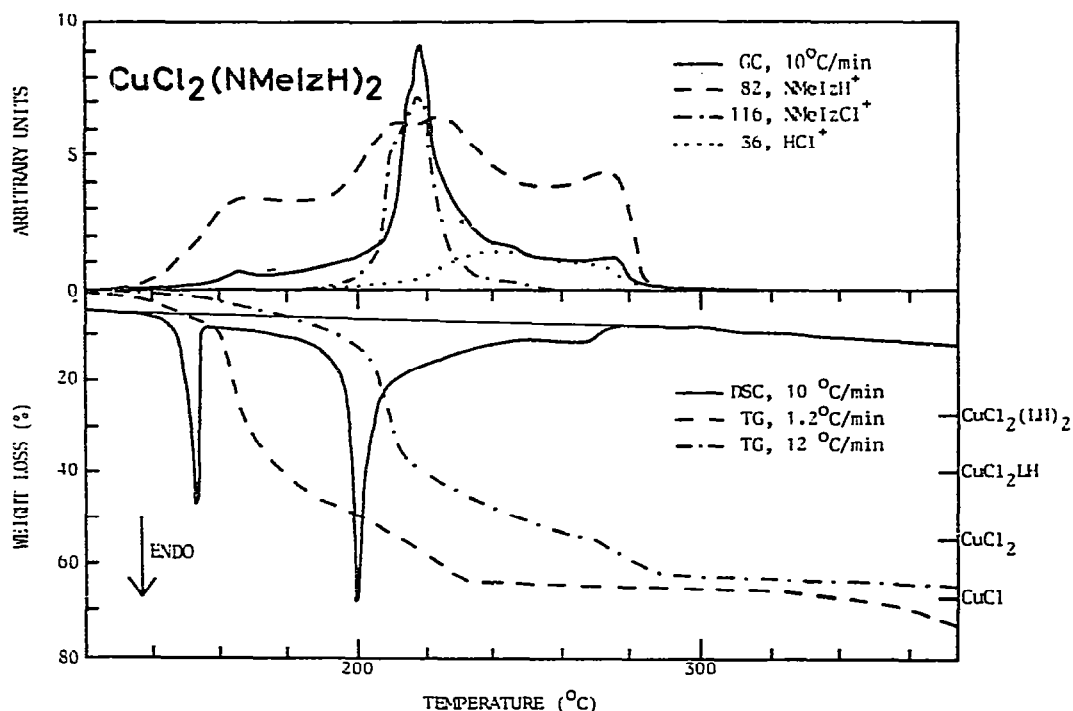


Fig. 1. Thermal decomposition of CuCl<sub>2</sub>(NMeIzH)<sub>2</sub>. GC and EGA curves at a heating rate of 10°C min<sup>-1</sup> (upper part), DSC and TG curves at different heating rates (lower part). The compound decomposes in the liquid phase after melting at 152°C.

With increasing temperature the compound decomposes in the liquid phase, first giving free ligand in the gas phase and probably solid  $\text{CuCl}_2 \cdot (\text{NMeIzH})$  according to reaction (2). This is confirmed by the high-temperature X-ray photograph of  $\text{CuCl}_2(\text{NMeIzH})_2$ . At about  $195^\circ\text{C}$  the rate of decomposition increases, while the gas phase mainly consists of free ligand and chlorinated ligand along with a small amount of  $\text{HCl}$ , considering the GC peak in the upper part of Fig. 1 and the great loss of weight between  $200$  and  $210^\circ\text{C}$  at a heating rate of  $12^\circ\text{C min}^{-1}$ . This can be explained by the occurrence of the reduction of  $\text{Cu(II)}$  to  $\text{Cu(I)}$  by the ligand according to reactions (3) and (4). The chloride anion cannot be the reducing agent, because no  $\text{Cl}_2$  was detected by the mass spectrometer.

During the whole decomposition process free *N*-methyl imidazole is released, but the reduction—oxidation reaction (around  $200^\circ\text{C}$ ) is chiefly responsible for the greater part of the complete decomposition. From Fig. 1 it can be seen that  $\text{HCl}$  is formed after the formation of  $\text{LCl}$ . This can be explained by the formation of a complex like  $[\text{LH}_2]^+[\text{CuCl}_2]^-$  during the reduction oxidation reaction, hampering the release of the  $\text{HCl}$ , according to reaction (4). This  $\text{HCl}$  gas is released at higher temperatures according to reaction (5).

At ca.  $270^\circ\text{C}$  the DSC curve shows a weak endothermic effect caused by release of pure ligand. This is confirmed by the last part of the GC and EGA curve of the ligand and also by the TG curve in the temperature region  $270$ — $290^\circ\text{C}$  (heating rate  $12^\circ\text{C min}^{-1}$ ).

The residue at  $300^\circ\text{C}$  primarily consists of  $\text{CuCl}$  and a certain amount of  $\text{CuCl}_2$ . No accurate quantitative prediction can be made about the amounts of  $\text{CuCl}$  and  $\text{CuCl}_2$  as the conditions of the decomposition (sample weight, heating rate, velocity of the gas stream, etc.) strongly influence the rate and temperature of decomposition of the compound. Heating above  $300^\circ\text{C}$  causes sublimation of  $\text{CuCl}$  and  $\text{CuCl}_2$  and further decomposition into metallic copper and chlorine.

In Figs. 1—4 results obtained from different techniques for all *N*-methyl imidazole compounds have been compiled with the temperature axis in common. In consequence of great differences in geometry and other experimental conditions, corresponding reactions may not be in entire temperature agreement. The temperatures of the GC/EGA experiments, for example, were determined by measuring the temperature in the furnace. As a result GC/EGA curves must be slightly shifted to lower temperatures to obtain the sample temperatures with respect to the DSC data.

The great influence of the heating rate during decomposition may be demonstrated by the two TG curves at  $12^\circ\text{C min}^{-1}$  and  $1.2^\circ\text{C}$  in Fig. 1. When comparing results obtained from different instruments, this effect should also be taken into account. In the remaining part of this paper only TG curves obtained at  $12^\circ\text{C min}^{-1}$  are discussed.

Since the character of the decomposition reactions is rather complex, it was impossible to determine the bond strength of the ligand to the central copper ion. Only the overall enthalpy of the decomposition of  $\text{CuCl}_2(\text{NMeIzH})_2$  to  $\text{CuCl}$  and  $\text{CuCl}_2$  is found to be  $124 \pm 4 \text{ kJ mole}^{-1}$ .

Figure 2 shows the thermal decomposition of  $\text{CuCl}_2(\text{NMeIzH})_4$ . The com-

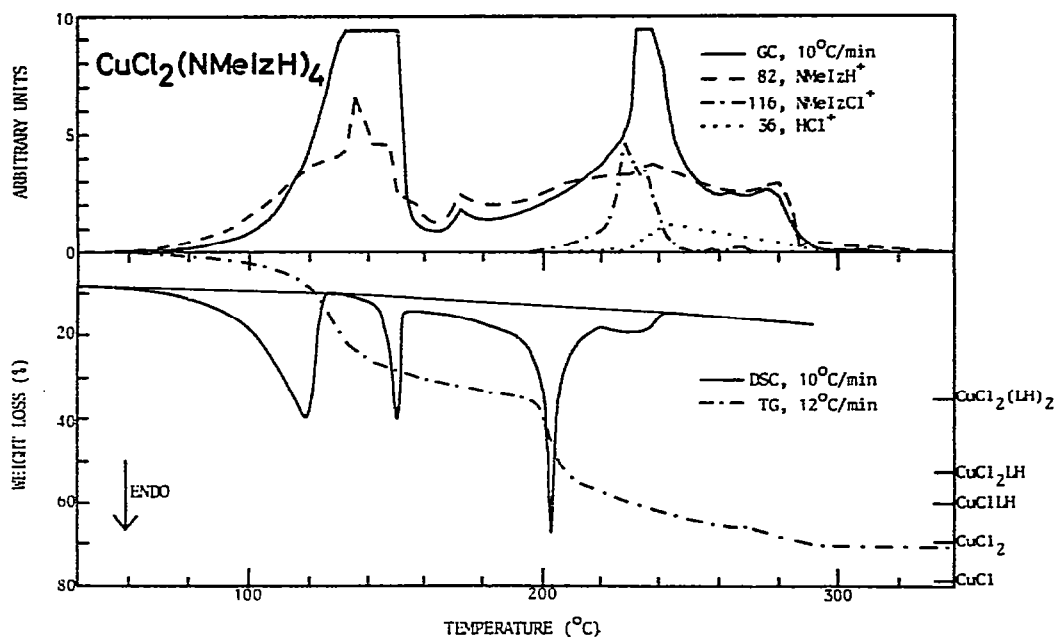


Fig. 2. Thermal decomposition of  $\text{CuCl}_2(\text{NMeIzH})_4$ . GC and EGA curves at a heating rate of  $10^\circ\text{C min}^{-1}$  (upper part), DSC and TG curves at different heating rates (lower part). The compound decomposes into  $\text{CuCl}_2(\text{NMeIzH})_2$  in the solid phase. Further heating shows a similar thermal behaviour as found for pure  $\text{CuCl}_2(\text{NMeIzH})_2$  (Fig. 1).

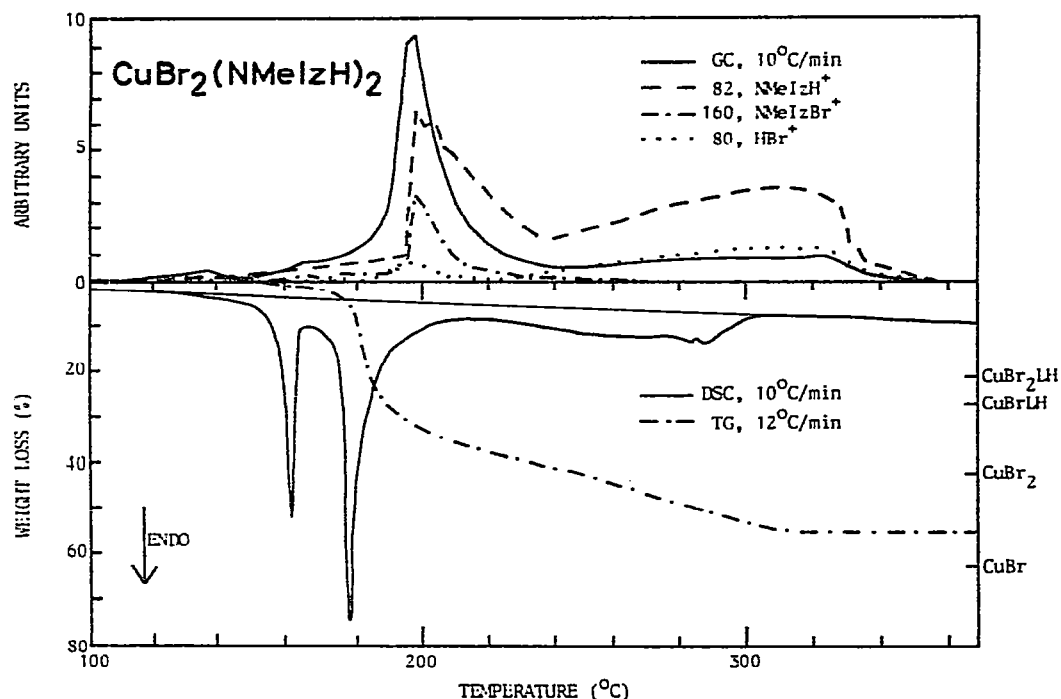


Fig. 3. Thermal decomposition of  $\text{CuBr}_2(\text{NMeIzH})_2$ . GC and EGA curves at a heating rate of  $10^\circ\text{C min}^{-1}$  (upper part), DSC and TG curves at different heating rates (lower part). During initial decomposition the compound melts at  $159^\circ\text{C}$ .

TABLE 1

Temperatures ( $T$ ), temperature ranges ( $\Delta T$ ) and heats of decomposition and melting ( $\Delta H$ ) of Cu(II) imidazole and *N*-methyl imidazole compounds measured by DSC

Compound	Temperatures ( $^{\circ}\text{C}$ )			$\Delta H$ values ( $\text{kJ mole}^{-1}$ ) <sup>a</sup>				
	$\Delta T_{4 \rightarrow 2}$	$\Delta T_{2 \rightarrow 0}$	$T_{\text{melt}}$	$T_{\text{peak}}$ <sup>b</sup>	$\Delta H_{4 \rightarrow 2}$ <sup>c</sup>	$\Delta H_{2 \rightarrow 0}$ <sup>c</sup>	$\Delta H_{4 \rightarrow 0}$ <sup>c</sup>	$\Delta H_{\text{melt}}$ <sup>d</sup>
CuCl <sub>2</sub> (NMeIzH) <sub>2</sub>		120–285	152	197		62 (4)		16 (1)
CuCl <sub>2</sub> (NMeIzH) <sub>4</sub>	60–130	130–247	152	204	49 (2)	68 (3)	58 (3)	15 (1)
CuBr <sub>2</sub> (NMeIzH) <sub>2</sub>		128–310	159	174		75 (2)		19 (1)
CuBr <sub>2</sub> (NMeIzH) <sub>4</sub>	80–163	163–296	159	171	62 (1)	54 (1)	58 (1)	11 (5)
CuCl <sub>2</sub> (IzH) <sub>2</sub>		151–317		193		64 (3)		
CuCl <sub>2</sub> (IzH) <sub>4</sub>	125–360 <sup>e</sup>			207			67 (5)	
CuBr <sub>2</sub> (IzH) <sub>2</sub>		125–385	160	208		72 (3)		16 (1)
CuBr <sub>2</sub> (IzH) <sub>4</sub>	150–235	235–390		221	57 (4)	62 (4)	59 (4)	

<sup>a</sup> Standard deviations are indicated in parentheses.

<sup>b</sup> Temperature of maximum decomposition rate.

<sup>c</sup> Expressed in  $\text{kJ mole}^{-1}$  ligand.

<sup>d</sup> Expressed in  $\text{kJ mole}^{-1}$  compound.

<sup>e</sup> Temperature range according to the overall decomposition ( $4 \rightarrow 0$ ).

compound first decomposes into  $\text{CuCl}_2(\text{NMeIzH})_2$  in the solid phase in the temperature range of  $60\text{--}130^\circ\text{C}$ , as can be seen from the DSC curve. This is confirmed by the mass spectrogram and the TG curve. Assuming that the mentioned decomposition is complete at  $130^\circ\text{C}$  (DSC curve) — which might not be exactly the case — the enthalpy of the reaction is found to be  $97 \pm 3 \text{ kJ mole}^{-1}$ . Further heating shows a similar thermal behaviour as found for pure  $\text{CuCl}_2(\text{NMeIzH})_2$  (see above). The overall enthalpy of the decomposition of solid  $\text{CuCl}_2(\text{NMeIzH})_4$  to  $\text{CuCl}$  and  $\text{CuCl}_2$  is found to be  $234 \pm 5 \text{ kJ mole}^{-1}$ .

The thermal behaviour of  $\text{CuBr}_2(\text{NMeIzH})_2$  (see Fig. 3) bears a great resemblance to that of the corresponding chloride compound. Melting temperature, heat of melting and the overall enthalpy of the decomposition are listed in Table 1.

The TG curve of the decomposition of  $\text{CuBr}_2(\text{NMeIzH})_4$  (see Fig. 4) does not show separate steps on heating. Probably  $\text{CuBr}_2(\text{NMeIzH})_2$  is formed as an intermediate product during the decomposition. The latter compound melts at  $159^\circ\text{C}$ , i.e. before the complete conversion of  $\text{CuBr}_2(\text{NMeIzH})_4$  into  $\text{CuBr}_2(\text{NMeIzH})_2$ , while the reduction of  $\text{Cu(II)}$  is initiated according to eqns. (3) and (4). Further heating shows a similar thermal behaviour as found for pure  $\text{CuBr}_2(\text{NMeIzH})_2$ .

The existence of  $\text{CuBr}$  as a reduction product of both the brominated coordination compounds is proved by the occurrence of a DSC peak at  $477^\circ\text{C}$  (not shown in the figures), which corresponds to a solid state transition of  $\text{CuBr}$ .

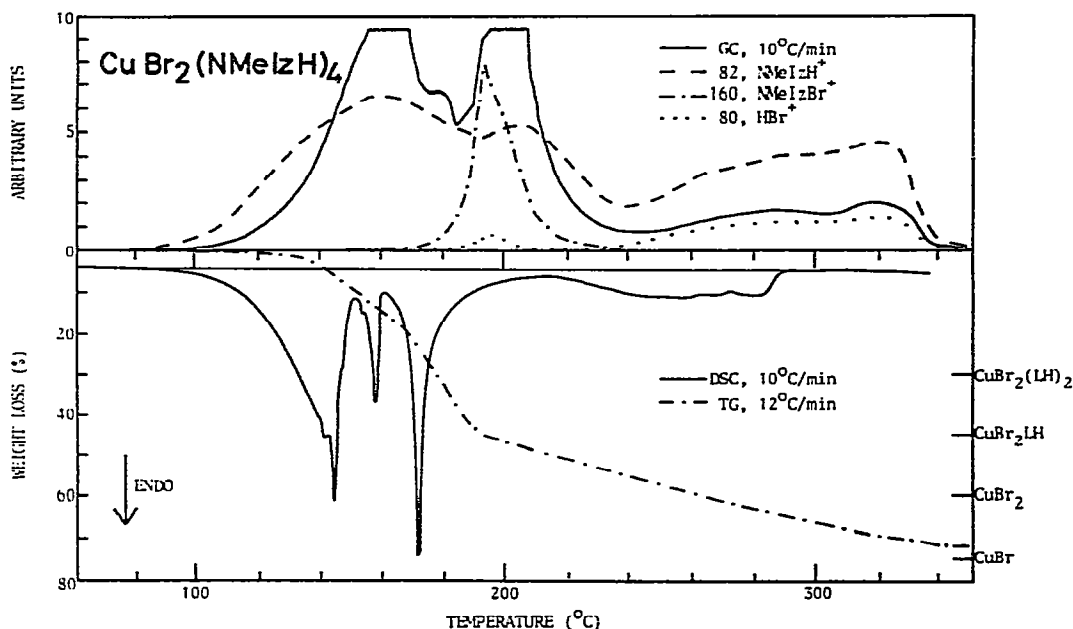


Fig. 4. Thermal decomposition of  $\text{CuBr}_2(\text{NMeIzH})_4$ . GC and EGA curves at a heating rate of  $10^\circ\text{C min}^{-1}$  (upper part), DSC and TG curves at different heating rates (lower part). Before complete decomposition of  $\text{CuBr}_2(\text{NMeIzH})_4$  into  $\text{CuBr}_2(\text{NMeIzH})_2$  the latter compound melts ( $159^\circ\text{C}$ ) and decomposes into  $\text{CuBr}_2$  and  $\text{CuBr}$  on further heating.



### Imidazole compounds

As can be seen from Figs. 5–8 the thermal decomposition of Cu(II) imidazole compounds is much more complex than found for the *N*-methyl imidazole compounds. As a general result only the overall decomposition enthalpies could be determined; these are also listed in Table 1.

The GC and EGA curves of  $\text{CuCl}_2(\text{IzH})_2$  and  $\text{CuCl}_2(\text{IzH})_4$  show a similar thermal behaviour as described above by eqns. (3)–(5). The high-temperature Guinier–De Wolff X-ray photograph of  $\text{CuCl}_2(\text{IzH})_2$  indicated that, after melting of the compound, solid CuCl was formed. This is confirmed by the solid state transition peaks at 407 and 417°C of the DSC curve (see Fig. 5).

The thermal decomposition of  $\text{CuCl}_2(\text{IzH})_4$  is presented in Fig. 6. Considering the pattern of the X-ray powder photograph it can be concluded that solid  $\text{CuCl}_2(\text{IzH})_4$  is gradually converted into solid  $\text{CuCl}_2(\text{IzH})_2$ . On further heating the latter compound decomposes in the solid phase according to eqn. (2). After melting CuCl was formed due to the reduction of Cu(II) to Cu(I).

Figure 7 shows the thermal decomposition of  $\text{CuBr}_2(\text{IzH})_2$ . No EGA curves could be obtained above 320°C due to the limitations of the furnace with the mass spectrometer. The compound melts at 160°C having  $\Delta H = 16 \pm 1 \text{ kJ mole}^{-1}$ , with an initial loss of ligand. On further heating more imidazole is released while Cu(II) is reduced to Cu(I) as described by eqn. (4).

Figure 8 shows the decomposition of  $\text{CuBr}_2(\text{IzH})_4$ . The high-temperature

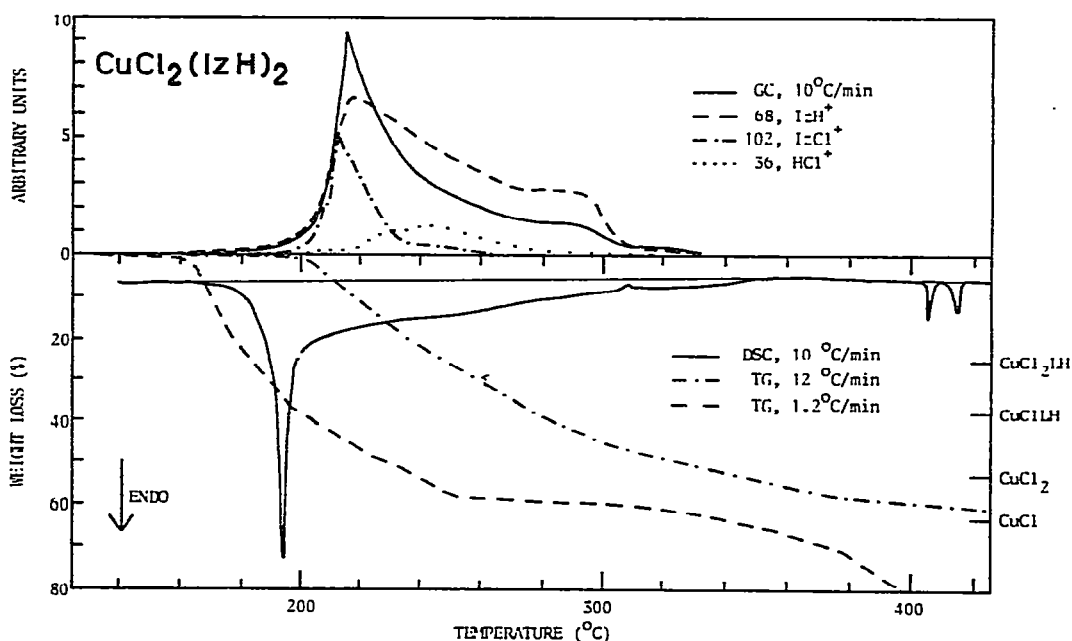


Fig. 5. Thermal decomposition of  $\text{CuCl}_2(\text{IzH})_2$ . GC and EGA curves at a heating rate of  $10^\circ\text{C min}^{-1}$  (upper part), DSC and TG curves at different heating rates (lower part). The peaks at  $407^\circ\text{C}$  and  $417^\circ\text{C}$  are solid state transitions of CuCl.

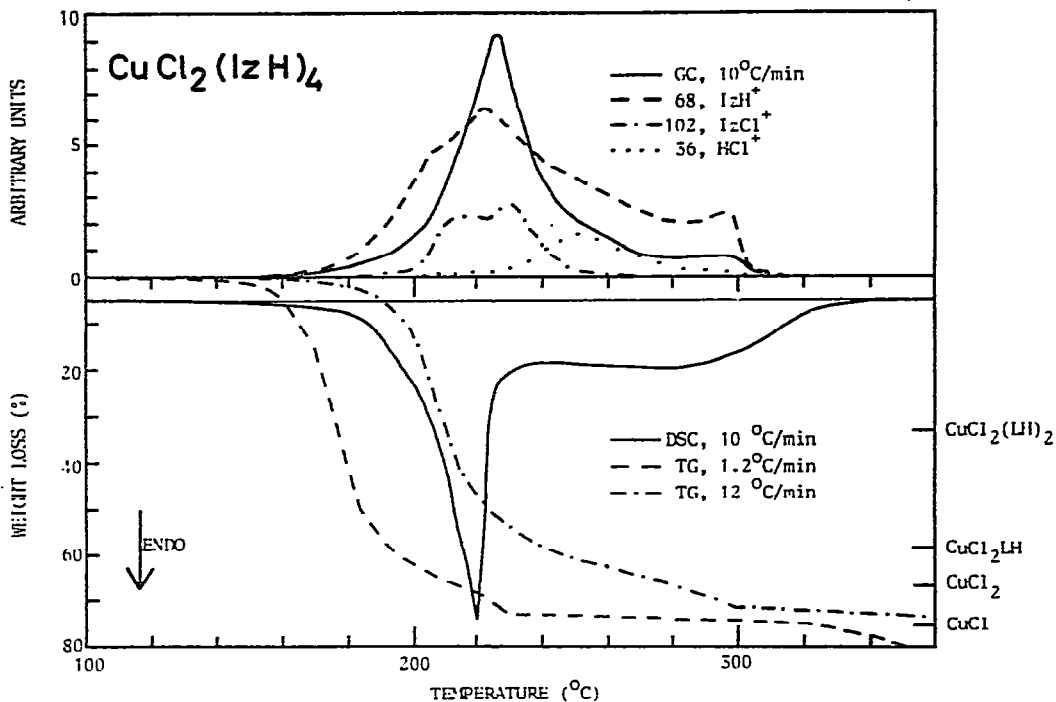


Fig. 6. Thermal decomposition of  $\text{CuCl}_2(\text{IzH})_4$ . GC and EGA curves at a heating rate of  $10^\circ\text{C min}^{-1}$  (upper part), DSC and TG curves at different heating rates (lower part). At  $407^\circ\text{C}$  and  $417^\circ\text{C}$  transitions of solid  $\text{CuCl}$  have been observed but are not shown here.

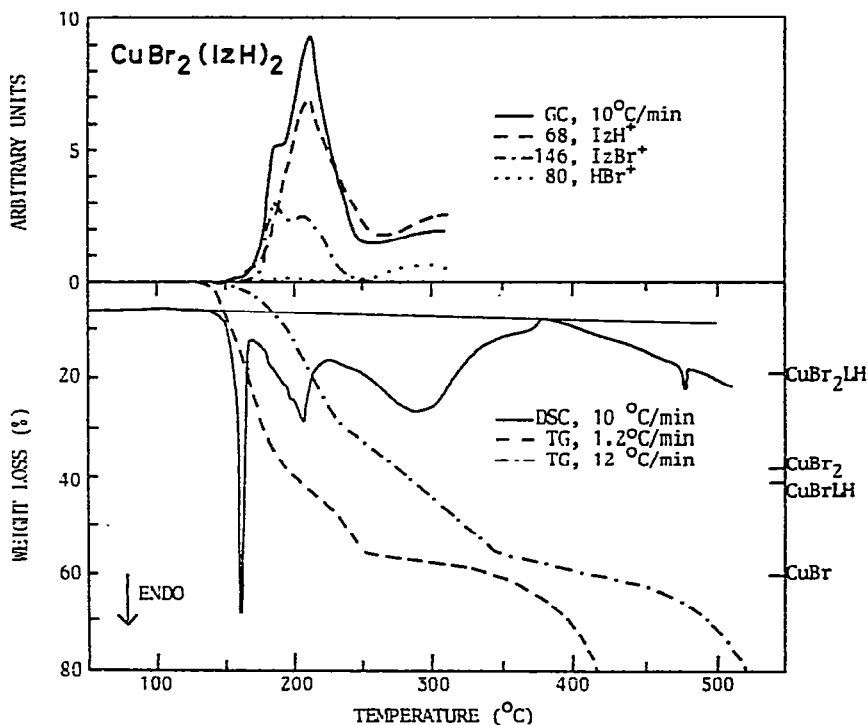


Fig. 7. Thermal decomposition of  $\text{CuBr}_2(\text{IzH})_2$ . GC and EGA curves at a heating rate of  $10^\circ\text{C min}^{-1}$  (upper part), DSC and TG curves at different heating rates (lower part). The compound melts at  $160^\circ\text{C}$ . During the decomposition a transition peak of  $\text{CuBr}$  has been determined at  $477^\circ\text{C}$ .

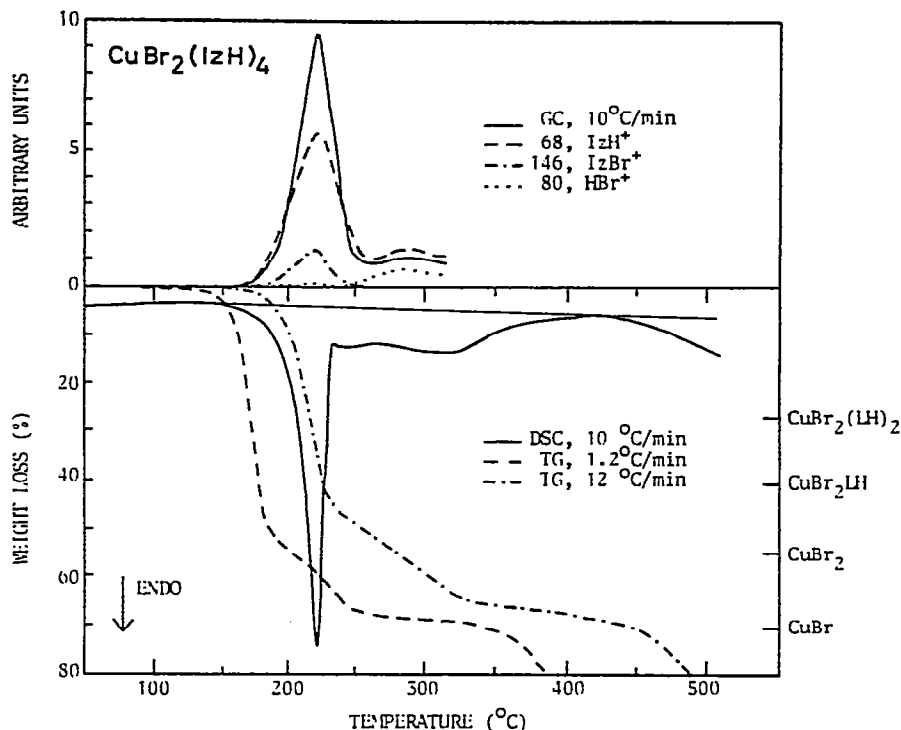


Fig. 8. Thermal decomposition of  $\text{CuBr}_2(\text{IzH})_4$ . GC and EGA curves at a heating rate of  $10^\circ\text{C min}^{-1}$  (upper part), DSC and TG curves at different heating rates (lower part). No separate melting point for  $\text{CuBr}_2(\text{IzH})_2$  has been found at  $160^\circ\text{C}$ .

X-ray photograph of this compound did not show the presence of solid  $\text{CuBr}_2(\text{IzH})_2$ , due to its lower melting point. Further heating shows a similar thermal behaviour as found for  $\text{CuBr}_2(\text{IzH})_2$ .

#### FINAL REMARKS

In most cases it appeared to be impossible to obtain exact thermodynamic data for Cu(II) imidazole and *N*-methyl imidazole compounds. The heats of the overall decomposition reactions are small compared with the results obtained by Van Dam et al. [10] for Ni(II) imidazole and *N*-methyl imidazole compounds. This can be explained by the complex character of the decomposition of the observed compounds [see eqns (3)–(5)]. In particular the reduction of Cu(II) by the ligands causes unknown heat effects which can greatly influence the overall enthalpy of the decomposition reactions. The temperatures and heats of melting of most Cu(II) *N*-methyl imidazole compounds could be determined with a fairly high degree of accuracy.

#### ACKNOWLEDGEMENTS

The authors wish to thank J.C. van Dam for helpful discussions and J.H.F. Grondel for technical advice. We are indebted to Drs. B. van de Graaf and

P.J.W. Schuyl and Mrs. A.H. Knol-Kalkman for cooperation in analyzing the samples by mass spectroscopy and N.M. van der Pers and J.F. van Lent for performing and interpreting the high-temperature X-ray photographs. Thanks are owed to J. van Willigen for drawing the figures and Miss M.J.A. Wijnen for typing the manuscript.

#### REFERENCES

- 1 J.S. Richardson, K.A. Thomas, B.H. Rubin and D.C. Richardson, *Proc. Natl. Acad. Sci. U.S.A.*, 72 (1975) 1349.
- 2 For a review see: F. Basolo, B.M. Hoffman and J.A. Ibers, *Acc. Chem. Res.*, 8 (1975) 384.
- 3 For a review see: J.P. Collman, *Acc. Chem. Res.*, 10 (1977) 265.
- 4 R.F. Salemme, J. Kraut and M.D. Kamen, *J. Biol. Chem.*, 248 (1973) 7701.
- 5 For a review see: R.J. Sundberg and R.B. Martin, *Chem. Rev.*, 74 (1974) 471.
- 6 J. Reedijk, *Rec. Trav. Chim.*, 88 (1969) 1451.
- 7 A. Santoro, A.D. Mighell, M. Zocchi and C.W. Reimann, *Acta Crystallogr., Sect. B*, 25 (1969) 842.
- 8 H.M.J. Hendriks and J. Reedijk, *Rec. Trav. Chim.*, 98 (1979) 95.
- 9 J. Reedijk and G.C. Verschoor, *Acta Crystallogr., Sect. B*, 29 (1973) 721.
- 10 J.C. Van Dam, G. Hakvoort, J.C. Jansen and J. Reedijk, *J. Inorg. Nucl. Chem.*, 37 (1975) 713.
- 11 P.S. Gomm, A.E. Underhill and R.W.A. Oliver, *J. Inorg. Nucl. Chem.*, 34 (1972) 1879.
- 12 M.C. Navarro Ramsinger, M. Gayoso Andrade, *J. Therm. Anal.*, 14 (1978) 281.
- 13 G. Hakvoort, J.C. Van Dam and J. Reedijk, *Thermal Analysis, Proc. 5th ICTA, Kyoto, 1977*, p. 186.
- 14 J.A.C. van Ooyen and J. Reedijk, *J. Chem. Soc., Dalton Trans.*, (1978) 1170.
- 15 B.K.S. Lundberg, *Acta Chem. Scand.*, 26 (1972) 3977.
- 16 D.M.L. Goodgame, M. Goodgame and G.W. Rayner Cantram, *Inorg. Chim. Acta*, 3 (1969) 339.
- 17 G. Hakvoort, *Thermal Analysis, Proc. 4th ICTA, Budapest, 1 (1974) 469*.
- 18 Joint Committee on Powder Diffraction Standards, *Powder Diffraction File, Pennsylvania, 1978*.